HortScience 60(7):1075–1083. 2025. https://doi.org/10.21273/HORTSCI18428-24

Transformations of Nitrate, Ammonium, and Urea When Applied to Pine Bark-based Substrate

Forrest J. Brown
School of Plant and Environmental Sciences, Virginia Tech, Blacksburg, VA 24061, USA

James S. Owen Jr
US Department of Agriculture, Agriculture Research Service, Application Technology Research Unit, Wooster, OH 44691, USA

Alex X. Niemiera
School of Plant and Environmental Sciences, Virginia Tech, Blacksburg, VA 24061, USA

Keywords. container crops, denitrification, nitrification, nitrifier, nitrogen, soilless substrate, urea hydrolysis

Abstract. **Nitrogen (N) cycling and transformations remain topics of interest in crop production to determine the efficiency of applied mineral N. However, aspects of N cycling in agriculture that are often overlooked are the associated N cycle reactions and transformations based on applied N forms to horticultural crops produced in containers using soilless culture. This research aimed to conduct a fundamental investigation to gain a better understanding of how individual N sources react after being applied to a soilless substrate (pine bark). To accomplish these objectives, we identified N cycle processes by measuring aqueous and gaseous intermediate N forms to determine enzymatic and microbial-mediated processes after a single application of three distinct N sources [urea (CH_4N_2O-N), ammonium (NH_4^+-N), or nitrate (NO_3^--N)]. We conducted these experiments during two pseudo-replicated studies using the predominate production systems in specialty crop production in the United States (open-wall high tunnel to simulate open-air nursery production or controlled environment glass greenhouse). No notable differences were observed between the two production systems. Our results indicate that a sequential set of reactions occur based on the applied N source (urea hydrolysis, nitrification, and denitrification) and trend toward complete denitrification and the production of N_2 gas via major N cycle processes. These data also imply that CH_4N_2O-N, which is the least expensive N source, emits higher concentrations of reactive nitrogen (RN) gaseous species, predominately nitrous oxide (N_2O) and nitric oxide (NO), compared with the NO_3^--N source in the substrate aqueous phase. The NH_4^+-N source produces the same RN emissions as those when applying CH_4N_2O-N and NO_3^--N. Findings of this research suggest that CH_4N_2O-N may be preferred by growers based on associated costs, but increased inefficiency compared with NO_3^--N-based products may exist. Furthermore, these data suggest that higher RN emissions occur during hydrolysis of CH_4N_2O to NH_4^+ and during the nitrification of NH_4^+ to NO_3^-, more so than that during denitrification from NO_3^- to N_2. We hypothesized that N transformations can be determined by measuring substrate pore water and gaseous emissions during N transformation and harvesting plant tissue and substrate before and after N source applications.**

Commercial nitrogen (N) fertilizer practices typically result in significant losses (unused by plants) of this economically and environmentally impactful nutrient (Matassa et al. 2023). However, N fertilizer is a major and costly mineral nutrient input that is required throughout crop production worldwide (Chen and Wei 2018). Aqueous and gaseous emissions are the two major N loss avenues that contribute to inefficiency (Govindasamy et al. 2023). Aqueous losses of N in agricultural settings can include ammonium (NH_4^+-N), nitrite (aqueous NO_2-N), nitrate (NO_3^--N), and urea (CH_4N_2O-N). Nitrate (NO_3^--N) is a key runoff component in eutrophication and contaminant of aboveground and belowground aquifers (Wilson and Albano 2011). The sum of these aqueous N species constitutes dissolved inorganic N (DIN), which contributes to the total N of an aquatic system, altering the balance of aquatic organisms (Warsaw et al. 2012).

Gaseous fertilizer emissions include inert nitrogen gas (N_2-N), and noninert reactive N (RN) species comprising ammonia (NH_3), nitric oxide (NO), nitrous oxide (N_2O), or N dioxide (gaseous NO_2). The uncharged gaseous species N dioxide (NO_2-N) and negatively charged aqueous species nitrite (NO_2^--N) should not be confused. Agriculture is a major source of anthropogenic N_2O emissions worldwide (Kroeze et al. 1999), and gaseous RN species are contributors to atmospheric degradation and pollution. Nitrous oxide is a potent greenhouse gas with 298-times the global warming potential of carbon dioxide (CO_2) (Myhre et al. 2013). Nitric oxide is an upper ozone-degrading harmful air pollutant that impacts human health (Akiyama and Tsuruta 2003; US Environmental Protection Agency 2002). Both N_2O and NO are intermediary by-products of N fertilizer soil and microbial-mediated nitrification and denitrification reactions.

Literature about N use for the production of specialty crops (US Department of Agriculture term inclusive of ornamental, edible, and fruit-bearing horticultural crops) produced in open-air nurseries and controlled environment greenhouses when using soilless container-grown plant culture is incomplete. Basic and applied agricultural research of fertilizer N fate has been conducted primarily in mineral soil systems (Congreves et al. 2021; Govindasamy et al. 2023). In the United States, container-grown nursery crops are predominantly produced from liners (starter plants) in a greenhouse to finished plants in open-air nurseries using a porous pine bark-based substrate (Altland et al. 2018; Pokorny 1979) and have an economic impact within the United States of $13.8 billion (US Department of Agriculture–National Agricultural Statistics Service 2020).

Container-grown N research to date has primarily focused on container type (Million and Yeager 2022), irrigation application (Alam et al. 2009; Li et al. 2019), fertilizer rate and placement (Hoskins et al. 2014a; Majsztrik et al. 2010), and other best management practices (Bilderback et al. 2015; Mack et al. 2017; Zheng 2018). Fertilizer N applications generally consist of varying ratios of CH_4N_2O-N, NH_4^+-N, or NO_3^--N and vary by crop and production region. The concomitant and varied N transformations in the substrate after applying CH_4N_2O-N, NH_4^+-N, and NO_3^--N have not been thoroughly investigated.

Containerized cropping system research has shown that N cycle processes include CH_4N_2O hydrolysis (Niemiera et al. 2014), nitrification (Niemiera and Wright 1987a, 1987b), and denitrification (Havlin et al. 2014) that can occur within hours after N is applied to the container. Ubiquitous microbial communities and naturally available enzymes populate the container system and transform applied N into various aqueous (NO_2^--N and NH_4^+-N) and gaseous (NO-N, N_2O-N, NO_2-N, and NH_3-N) intermediaries and ultimate endpoints (N_2-N or NO_3^--N) being emitted from the container system (Galloway et al. 2004). Aqueous NO_3^--N and NH_4^+-N occur in the substrate solution and are assimilated in ratios for proper growth and development (Marschner 2012). The resulting holistic processes and resulting N species formations have been poorly documented in container culture.

Accounting for N fate within the container system is confounded by constrained water and nutrient storage and significant diurnal flux of nutrient solution resulting from crop water use and daily irrigation practices (Warsaw et al. 2012) or rain events throughout production. A steep vertical moisture gradient ranging from the upper substrate surface to

Downloaded from https://prime-pdf-watermark.prime-prod.pubfactory.com/ at 2025-08-15 via Open Access. This is an open access article distributed under the CC BY-NC license (https://creativecommons.org/licenses/by-nc/4.0/). https://creativecommons.org/licenses/by-nc/4.0/

the container bottom (Bilderback and Fonteno 1987) occurs because of interactions of gravity and substrate pore size (Hoskins et al. 2014b). The vertical moisture gradients of the container range from an aerobic condition in the top portion of the container and a combination of aerobic and anaerobic conditions at the bottom of the container (i.e., zone of saturation) following irrigation or rain and depending on root growth throughout the substrate.

The combination and ever-changing aerobic and anaerobic conditions of the container substrate and fertilizer applications coupled with diurnal changes in nutrient availability result in multiple concurrent N cycle processes. Thus, the dynamic substrate N processes are driven by urease ubiquity, microbial communities, root exudates, carbon contributed from the substrate, and high substrate temperatures that have been reported to exceed 50 °C on the south-facing wall throughout production (Arnold and McDonald 2006). The combination of intrinsic and extrinsic factors creates a diverse system for CH_4N_2O hydrolysis, nitrification, and denitrification reactions to proceed akin to N transformations rapidly observed across varying mineral soil systems that experience various moisture and temperature fluxes (Theis et al. 2019).

We aimed to determine the transformations of three individual N fertilizer sources (CH_4N_2O-N, NH_4^+-N, or NO_3^--N) when applied to an established container-grown crop produced in a commercial high tunnel (polyethylene-covered hoop house) or glass greenhouse. We hypothesized that N transformations can be determined by measuring substrate pore water and gaseous emissions during N transformation and plant and substrate N before and after applications.

Materials and Methods

High-tunnel simulated open-air nursery

Site description. The two-factor experiment (N source and time) was conducted from 9 to 11 Aug 2022 at the US Department of Agriculture–Agriculture Research Service, Application Technology Research Unit in Wooster, OH, USA (lat. 40°46′26.0″N, long. 81°54′42.6″W) in an open-wall, polyethylene-covered hoop house (i.e., high tunnel) to exclude rain (Supplemental Figs. 1 and 2). The N sources were arranged in a randomized block design.

Plant material and potting. At Last® *Rosa* × 'HORCOGJIL' (USPP 27,451; Rosaceae family) liners (224; Griffin Greenhouse Supplies, Inc., Tewksbury, MA, USA) were received and held in an open-wall, polyethylene-covered hoop house that received daily irrigation until planting. On 23 May 2022, shrub rose liners were pruned to similar sizes before planting to ensure experimental unit uniformity; then, an individual plant was transplanted in a #2 trade container (5.68 L volume × 21.6 cm height × 22.9 cm width; C600; Nursery Supplies Inc., Chambersburg, PA, USA) with a pine bark substrate (T.H. Blue Inc., Eagle Springs, NC, USA). The pine bark substrate was amended with 1.8 $kg \cdot m^{-3}$ ground dolomitic lime [95.0% $CaCO_3$ equivalent, 21.6% calcium (Ca), 10.0% magnesium (Mg); Soil Doctor, Atlanta, GA, USA] and 0.45 $kg \cdot m^{-3}$ granular micronutrient fertilizer [6.0% Ca, 3.0% Mg, 12.0% sulfur (S), 0.1% boron (B), 1.0% copper (Cu), 17.0% iron (Fe), 2.5% manganese (Mn), 0.1% molybdenum (Mo), 1.0% zinc (Zn); Micromax; Everris, Dublin, OH, USA). Pine bark was mixed with amendments in a ribbon mixer for 10 min [Twister I (single phase); Bouldin and Lawson, McMinnville, TN, USA] to uniformly incorporate amendments into the substrate.

Plant establishment. Shrub roses were grown for 7 weeks before experimental initiation (Fig. 1) to allow for establishment of the microbiome comparable to that of common production conditions and practices within the specialty crop industry. During this establishment period, plants received daily predawn (6:00 AM) irrigation delivered by pressure-compensated plum spray stakes (SKU 22500-002030; Netafim, Orbia Inc., Hatzerim, Israel). Approximately every 2 to 3 d, fertigation was applied to plants at 150 $mg\text{-}N \cdot L^{-1}$ with a complete water-soluble fertilizer (20N–5P_2O_5–20K_2O; 8% NH_4-N, 8% NO_3-N, 4% Urea-N; SKU 200285; Turf 2; Harrells LLC, Lakeland, FL, USA) as needed using a fertilizer injector (Dosatron D14MZ2; Ingersoll Rand, Davidson, NC, USA) from a stock solution at a 1:100 dilution, which is a typical practice of nursery production in the eastern United States. Two weeks before initiation of the experiment, plants were fertigated with 100 $mg \cdot L^{-1}$ potassium nitrate (KNO_3) using a 1:100 diluted stock solution using a dosing pump. The week before initiation of the experiment, the plants were irrigated with water without fertilizer to flush any freely available residual DIN from the experimental units. No nutritional deficiencies of model crop were noted during establishment and experimentation.

Nitrogen source and application. The three N source treatments were CH_4N_2O-N (SKU U20225; Research Products International, Mount, Prospect, IL, USA), NH_4^+-N applied as ammonium phosphate monobasic [$(NH_4)H_2PO_4$] (SKU A684-3; Thermo Fisher Scientific Inc., Waltham, MA, USA), and NO_3-N applied as KNO_3 (SKU P263-500; Thermo Fisher Scientific Inc.). Additionally, 2 L of 200 $mg \cdot L^{-1}$ of each N-containing solution was applied to each container; this dose was shown by Cavins et al. (2005) as sufficient for container crop production. Each N source was formulated by combining water with the N source agricultural salt to formulate treatments on 9 Aug 2022 as a single fertilization event; no further N application occurred for the remainder of the study (Fig. 1).

Substrate physical properties. Pine bark substrate physical properties (n = 4) were determined using the North Carolina State University porometer method (Fonteno and Harden 2010). Stabilized pine bark had a minimum air space of 29.7% by volume [standard error (*SEM*), ±1.2], maximum water holding capacity of 49.3% by volume (*SEM*, ±0.6), total porosity of 79.0% by volume (*SEM*, ±0.9), and a bulk density of 0.18 $g \cdot m^{-3}$ (*SEM*, ±0.1). Substrate texture (n = 3) was defined by the following three separate particle classes (Altland et al. 2014): coarse particles (diameter > 2.0 mm); medium particles (0.5 mm < diameter ≤ 2.0 mm); and fine particles (diameter < 0.5 mm). Particle size distribution was determined by mechanical agitation of oven-dried substrate for 5 min on a Ro-Tap shaker (Rx-29; W.S. Tyler, Mentor, OH, USA). Particle size distribution was determined by using sieves with appropriate mesh openings. Particle classes (by weight; *SEM*, ±0.1) were coarse (62.7%), medium (26.3%), and fine (11.0%).

Temperature. Daily air temperature data were obtained using a HOBO External Temperature/RH Sensor Data Logger (SKU MX2302A; Onset, Bourne MA). The average air temperature during this trial was 23.9 °C, with a maximum temperature of 36.5 °C and minimum temperature of 16.2 °C. Substrate temperature data were collected using HOBO Pendant MX Water Temperature Data Loggers (SKU MX2201; Onset) placed in the center of the containerized substrate. The average substate temperature during this trial was 23.7 °C, with a maximum temperature of 34.5 °C and minimum temperature of 17.8 °C (Supplemental Fig. 3).

Pore water extraction and N analysis. Pore water extractions (Fig. 1) occurred at 4, 8, 24, and 48 h after initiation (HAI) using the pour-through method (Wright 1986). In brief, we applied 180 mL of deionized water evenly over the substrate surface of each experimental unit (container; n = 4; total = 16). This process resulted in 40 to 60 mL of displaced pore water (substrate bulk solution). The displaced pore water was collected for analysis. Pore water was transferred into a labeled 50-mL conical tube (Falcon® 50-mL conical tube; Corning, Corning, NY, USA). Samples were separated and analyzed to determine electrochemical properties [pH and electrical conductivity (EC)]; mineral nutrient ions; and total organic N and carbon.

Additional deionized water was added to each experimental unit or container at 23 and 47 HAI to ensure the container was saturated

Received for publication 24 Dec 2024. Accepted for publication 12 Apr 2025.
Published online 13 Jun 2025.
We acknowledge Hannah Blice and Leslie Morris of the US Department of Agriculture–Agriculture Research Service (USDA-ARS) Application Technology Research Unit in Wooster, Ohio, USA, for technical expertise. We acknowledge The Ohio State University and Virginia Tech for facilities and support throughout the duration of these studies.
The authors declare no competing interest.
This research was conducted at the Application Technology Research Unit in Wooster Ohio and in part funded by the United States Department of Agriculture Agricultural Research Service, Crop Production Project 5082-21000-001-000D.
J.S.O. is the corresponding author. E-mail: deuteriumo18@gmail.com.
This is an open access article distributed under the CC BY-NC license (https://creativecommons.org/licenses/by-nc/4.0/).

Downloaded from https://prime-pdf-watermark.prime-prod.pubfactory.com/ at 2025-08-15 via Open Access. This is an open access article distributed under the CC BY-NC license (https://creativecommons.org/licenses/by-nc/4.0/). https://creativecommons.org/licenses/by-nc/4.0/

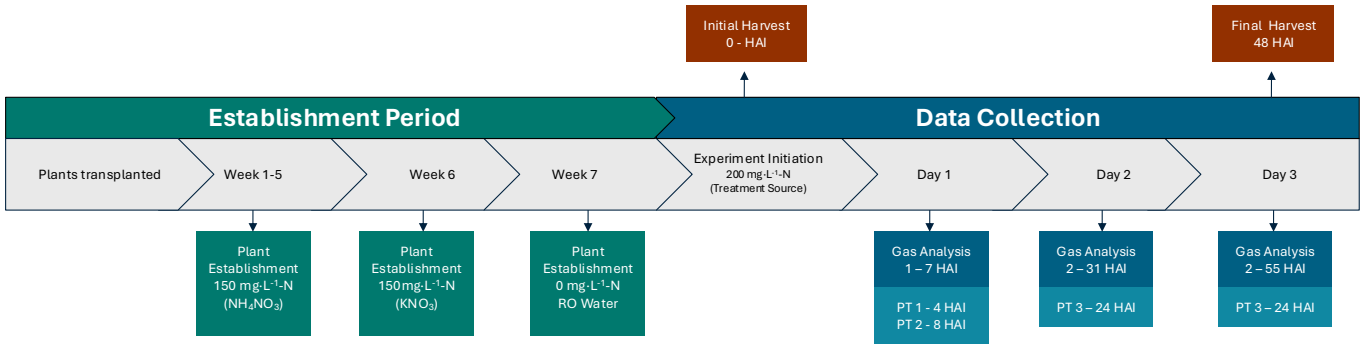

Fig. 1. Timeline including hours after initiation (HAI) of the establishment period including concentrations and sources of nitrogen (N) applied. Data collection period depicting N application, initial and final harvest, gas analysis, pour-through sampling (PT), and their respective times of collection are shown.

before conducting a pour-through, which requires containers to be at field capacity to obtain a representative sample of plant-available pore water (Wright 1986). Specifically, an additional 200 mL or 300 mL of deionized water was added to each container at 23 HAI and 47 HAI to bring containers to field capacity. At 15 min after application, leachate was collected and reapplied over the top of the substrate surface. Substrates were then allowed to freely leach for 45 min before pour through extraction.

Pore water sample pH was measured using a benchtop meter (MA235 pH/Ion Analyzer; Mettler Toledo, Columbus, OH, USA) with an InLab Expert PRO-ISM pH electrode (Mettler Toledo). The EC was measured using a benchtop conductivity meter (S230 SevenCompact; Mettler Toledo) with an InLab 741-ISM electrode (Mettler Toledo).

Extracted pore water aliquots were filtered with a 0.45-µm syringe filter (Choice™ nylon Syringe Filter; Thermo Fisher Scientific Inc.). A 7-mL aliquot of filtered solution was placed in a 10-mL polystyrene vial (074228; Thermo Fisher Scientific Inc.) for immediate ion chromatography analysis, 10 mL was placed in a 22.2-mL PTFE/SILicone ulined (824030-2385; Neta Scientific, Hainesport, NJ, USA) for an immediate total organic carbon (TOC)/dissolved organic carbon (DOC) total N (TN) analysis, and a 10-mL aliquot was placed in a 15-mL polypropylene vial (339650; Thermo Fisher Scientific Inc.). An additional aliquot was placed in a 10-mL round bottom borosilicate glass tube (14-961-27; Thermo Fisher Scientific Inc.) for urea analysis. The rest of the sample was frozen and stored at −20 °C for reanalysis if necessary.

Ion concentrations were determined via ion chromatography coupled with an AS-AP chilled autosampler (ICS6000; Thermo Fisher Scientific Inc.). An Ion Pac AS19 2-× 250-mm column (062886; Thermo Fisher Scientific Inc.) and Ion Pac CS12a 2-× 250-mm column (046075; Thermo Fisher Scientific Inc.) were used for anion analysis and cation analysis, respectively. Limits of detection of anions nitrite (NO_2^--N) and nitrate (NO_3^--N) and cation ammonium (NH_4^+-N) were 0.2 to 125 mg·L^{-1}. The TOC and TN (sum of organic and inorganic N forms) analyses via combustion were performed using a TOC and TN aqueous analyzer with ASI-L Autosampler (Shimadzu, Colombia, MD, USA) with a range of 0 to 100 mg·L^{-1}.

The urea-N analysis was performed using Method 10-206-00-1-A in deionized water using the Flow Injection Analysis System (Lachat Quikchem 8500; Hach Co., Loveland, CO, USA). Samples were diluted to suit detection limits of 0.1 to 20 mg·L^{-1} CH_4N_2O-N and analyzed in The Ohio State University Service Testing and Research laboratory (STAR Laboratory, Wooster, OH, USA). Diluted samples were reanalyzed immediately if not within detection limits for any measure.

Reactive N gas analysis. Gaseous emissions (Fig. 1) were sampled at 7, 31, and 55 HAI. A real-time gas analysis was conducted using Fourier transform infrared spectroscopy (FTIR; Terra GT5000; Gasmet, Vantaa, Finland). A closed-loop sampling system was made using a plastic 22.74-L bucket with polyurethane tubing (McMaster-Carr, Cleveland, OH, USA) that was connected to the FTIR apparatus. Chamber integrity was confirmed with CO_2 measurements during experimental sampling. One experimental unit (container with plant) was placed inside the chamber of the closed-loop system, and the gas flux was measured over 5 min (n = 4 per treatment). Then, the FTIR apparatus was returned to ambient gas concentrations for 3 min; ambient gas concentrations were sampled between each experimental unit. Gas flux on a per-container basis over time, $f_{N \cdot t}^{-1}$, was calculated using Eq. [1] (Gyawali et al. 2019).

$$f_{NOx} = \frac{P_0}{RT_0}\frac{V_c}{\Delta t}\frac{\Delta C}{\Delta t} \quad [1]$$

where P_0 is the pressure within the chamber [M·L^{-1}·t^{-2}], which is assumed to be equivalent to the atmospheric pressure, V_c is the cumulative volume of the chamber, apparatus internal volume, and tubing volume [L^3], R is the ideal gas law constant [M·L^2·N^{-1}·T^{-1}·t^{-2}], T_0 is the air temperature in kelvin (K) [T], ΔC is the change in concentration of a given gas on a molar basis [N·N^{-1}], Δt, which is then used to compare change in gaseous species concentration over change in time [t]. Gaseous species of interest included N_2O-N, NO-N, NH_3-N, NO_2-N, and the sum of all four N gases as RN. Observations of gaseous flux were stopped before head space saturation of each specific gas species to ensure flux calculations were not underestimating or overestimating gas flux. The FTIR apparatus was calibrated before the initiation of gas data collection for each sampling date.

Plant tissue and substrate N content. Initial and final harvest of aboveground and belowground biomass and substrate were performed before experiment initiation (0 HAI) and at 48 HAI to determine the N content of four plants per block, resulting in a total of 16 plants (Fig. 1). Roots were cut from shoots at the substrate surface and washed using a high-pressure water stream to remove substrate before drying. Shoot and root tissues were dried (60 °C) until no change in mass could be detected. Bark substrates were dried (100 °C) and weighed until no loss of mass could be detected. Plant tissues and substrates were weighed and then ground to pass through a 2-mm sieve using a laboratory mill (Foss Cyclotec™ 1093; Foss, Hillerød, Denmark). Once ground, plant tissue and substrate were placed in a labeled coin envelope and mailed to Brookside Laboratories (New Bremen, OH, USA) to determine the N content by combustion (T002 analysis). Plant tissue and substrate N contents were determined by dry weight × N concentration, and root and shoot N contents were combined to determine total plant N.

Statistical analysis and interpretation. Data were analyzed using JMP Pro 15.0 (SAS Institute, Inc., Cary, NC, USA). Distribution of all data were examined, and most were determined to have a normal distribution. If data were not normally distributed, then residuals, log, and cube root transformations were conducted to meet the assumptions of normal distribution. The N source and time were subject to a two-way analysis of variance. Pearson correlation coefficients ($R^2 > 0.4$) were used to determine relationships. $P \leq 0.05$ was used to determine statistical differences. Gaseous data were subject to a multivariate analysis of variance for repeated measures.

Controlled environment glass greenhouse

Site description. A glass greenhouse was used to evaluate the effects of a controlled environment (Supplemental Figs. 2 and 4). Unless otherwise stated, plant material and potting, plant establishment, N source, measures

Downloaded from https://prime-pdf-watermark.prime-prod.pubfactory.com/ at 2025-08-15 via Open Access. This is an open access article distributed under the CC BY-NC license (https://creativecommons.org/licenses/by-nc/4.0/). https://creativecommons.org/licenses/by-nc/4.0/

of substrate physical properties and temperature, pore water extraction, gas analysis, and data analysis and interpretation were the same as those used in the high tunnel experiment (Supplemental Fig. 4). The mean greenhouse daytime temperature was 24 °C and the mean greenhouse nighttime temperature was 18 °C while maintaining a 16-h photoperiod provided by sunlight with supplemental lighting delivered by high-pressure sodium and metal halide lamps (GLX/GLS e-systems GROW lights; PARsource, Petaluma, CA, USA) (Supplemental Fig. 5).

Roses were allowed to establish for 9 weeks in the high tunnel after potting. On 26 Aug 2022, plants were moved to a heated glass greenhouse to allow acclimation of experimental units for 3 weeks before experiment initiation. Plants were allowed to establish for 12, 13, or 14 weeks. The experiment timeline was as follows: NH_4-N was applied on 13 Sep 2022; data collection concluded on 15 Sep 2022; NO_3-N was applied on 20 Sep 2022; data collection concluded on 22 Sep 2022; CH_4N_2O-N was applied on the 27 Sep 2022; and data collection concluded on 29 Sep 2022. The staggered separation of each N source application reduced the amount of time between sample collection and analysis.

Fertigation was stopped before each N source application. Deionized water was the irrigation water source for 4 d before each N source application to remove pore water DIN. We were unable to analyze samples for TN because of analytical equipment failure; therefore, we excluded these data from analysis.

Results

High-tunnel simulated open-air nursery

The N source treatments were pooled over time (HAI) and N treatment for the plant N content (0.3 g) or dry weight (18.0 g) because of the lack of statistical differences (Supplemental Fig. 6).

Urea treatment

Aqueous pore water. Urea-N curvilinearly decreased ($P < 0.0001$; $R^2 = 0.74$) from 44.7 mg·L^{-1} at 4 HAI to 31.2 mg·L^{-1} at 8 HAI, and to 1.4 at 24 HAI (Fig. 2). By 48 HAI, CH_4N_2O-N was undetected in the extracted pore water. Ammonium-N exhibited a polynomial fit whereby concentrations averaged 3.0 mg·L^{-1} at both 4 HAI and 8 HAI, increased to 10.9 mg·L^{-1} at 24 HAI, and decreased to 6.3 at 48 HAI ($P = 0.0004$; $R^2 = 0.70$) (Fig. 2). Nitrite-N concentrations curvilinearly increased ($P < 0.0001$; $R^2 = 0.81$) throughout sampling from 0.4 mg·L^{-1} at 4 HAI to 7.4 mg·L^{-1} at 24 HAI and peaked (14.4 mg·L^{-1}) at 48 HAI. Nitrate-N exhibited a polynomial trend ($P = 0.0001$; $R^2 = 0.75$) whereby concentrations were initially low, averaging 1.8 mg·L^{-1} for the first 24 HAI; thereafter, they increased to 11.1 mg·L^{-1} at 48 HAI (Fig. 2). Total N concentrations decreased over the 48-h experimental duration and exhibited a polynomial trend, with a high initial value of 54.2 mg·L^{-1} that decreased to 23.4 mg·L^{-1} at 24 HAI ($P < 0.0001$; $R^2 = 0.81$) (Fig. 2). Total N remained stable for the final 24 h of the experiment (Fig. 2). Initial (4 HAI) pore water extract pH was 6.7, and it increased to 7.0 and 7.2 at 24 HAI and 48 HAI, respectively ($P = 0.0013$) (Fig. 3). The EC remained stable at approximately 0.8 mS·cm^{-1} over the 48-h experimental period (Fig. 3). The TOC concentration remained relatively stable throughout the experiment, averaging 54 mg·L^{-1} (Supplemental Fig. 7).

Gaseous emissions. There were no measured emissions of NH_3-N or NO_2-N gas after the application of CH_4N_2O-N (Fig. 2). Nitrous oxide-N emission exhibited a polynomial trend whereby concentrations increased from 0.2 at 7 HAI to 4.1 at 55 HAI ($P = 0.0007$; $R^2 = 0.80$) (Fig. 2). Nitric oxide-N emission increased from 0.6 μg·min^{-1} at 7 HAI to 7.4 μg·min^{-1} at 55 HAI ($P = 0.024$). Nitric oxide and nitrous oxide (NO-N and N_2O-N) were the two major contributors to RN emissions regardless of sampling time.

Ammonium treatment

Aqueous pore water. The aqueous NH_4^+-N concentration was highest at 14 mg·L^{-1} at the 4-HAI interval and decreased to 4.5 mg·L^{-1} at 48 HAI ($P = 0.0016$) (Fig. 2). Aqueous NO_2^--N increased linearly throughout the experiment ($P < 0.0001$; $R^2 = 0.78$) (Fig. 2). Nitrate-N was stable for the first 8 HAI and increased to 7.8 mg·L^{-1} at 48 HAI, exhibiting a linear trend ($P = 0.0022$; $R^2 = 0.50$) (Fig. 2). Total N concentrations remained stable throughout the experiment, with an average TN concentration of 19.5 mg·L^{-1}. Urea-N was not present in any samples. Pore water pH remained stable at 6.4, whereas EC had a decreasing polynomial fit ($P = 0.0328$; $R^2 = 0.41$) (Fig. 2) whereby values decreased from 1.1 to 0.9 mS·cm^{-1} over the experiment. The TOC increased linearly by 71% ($P = 0.0001$; $R^2 = 0.66$) over the 48-h sampling period (Supplemental Fig. 7).

Gaseous emissions. Two major contributors to RN emissions regardless of sampling time were NO-N and N_2O-N. Emissions of N_2O-N increased linearly from 0.2 μg·min^{-1} at 7 HAI to 1.9 μg·min^{-1} at 55 HAI ($P = 0.0012$; $R^2 = 0.67$) (Fig. 2). There were no differences in NO-N emissions during the 55-h span ($P = 0.8699$). A low emission of NH_3-N 0.1 μg·min^{-1} was detected at 7 HAI; thereafter, no NH_3-N emissions occurred for the remainder of experiment. Nitrogen dioxide-N was not detected at any sampling point during the experiment.

Nitrate treatment

Aqueous pore water. Aqueous NO_3^--N exhibited a decreasing polynomial fit ($P = 0.014$; $R^2 = 0.48$) (Fig. 2) whereby concentrations decreased from 93.8 mg·L^{-1} at 4 HAI to 58.3 mg·L^{-1} at 24 HAI. Nitrate-N concentrations remained stable for the final 24 h of sampling (Fig. 2). Nitrite-N remained low throughout all sampling, averaging less than 0.2 mg·L^{-1} pooled across all sample collections. Ammonium-N and CH_4N_2O-N remained below detection limits for all samples. Total N decreased from 90.1 mg·L^{-1} at 4 HAI to 68.6 mg·L^{-1} at 24 HAI and remained stable for the remainder of the trial ($P = 0.0018$). The pH of the pore water solution increased from 6.5 to 7.1 over the experiment ($P < 0.0001$) (Fig. 3). The EC values were higher than those of other N source treatments and decreased from 1.4 mS·cm^{-1} 4 HAI to 1.1 mS·cm^{-1} at 48 HAI ($P = 0.0002$), thus exhibiting a polynomial fit ($P < 0.0001$; $R^2 = 0.77$) (Fig. 3). The TOC concentrations (mg·L^{-1}) showed little change during the first 8 HAI; it decreased from 29 mg·L^{-1} to 28 mg·L^{-1} but increased during the remainder of the sampling points, with a final concentration of 42 mg·L^{-1} at 48 HAI ($P = 0.0008$) (Supplemental Fig. 7).

Gaseous emissions. Nitric oxide and N_2O (NO-N and N_2O-N) were the two major contributors to RN emissions regardless of sampling time. Gaseous N_2O-N and NO-N emissions remained stable at all sampling times throughout the experiment (Fig. 2). The application of NO_3^--N fertilizer resulted in the lowest RN emissions of all treatments across time. Emissions of NH_3-N and NO_2-N were not measured at any sampling point during experimental sampling.

Controlled environment glass greenhouse

Observations in the glass greenhouse were similar to those of the high tunnel. A notable difference is the first pore water extract (4 HAI) across all treatments showed little to no aqueous dissolved inorganic N across N sources. We attributed this to the initial extract consisting of primarily nondisplaced deionized water remaining in the zone of saturation at the time of N applications. Similar results were observed by Altland and Owen (2024).

Urea treatment

Aqueous pore water. Following the application of CH_4N_2O-N, the CH_4N_2O-N concentration was initially 0.1 mg·L^{-1} at 4 HAI and peaked at 30.4 mg·L^{-1} at 8 HAI; then, it decreased to 17.0 mg·L^{-1} at 24 HAI and 0.4 mg·L^{-1} at 48 HAI, thus exhibiting a polynomial fit ($P = 0.0341$; $R^2 = 0.41$) (Fig. 4). Ammonium-N concentration exhibited a polynomial trend with an initial concentration of 0.9 mg·L^{-1} at 4 HAI, increasing to 33.5 mg·L^{-1} at 8 HAI and 38.0 mg·L^{-1} at 24 HAI; thereafter, NH_4^+-N concentrations decreased to 19.1 mg·L^{-1} at 48 HAI ($P = 0.0045$; $R^2 = 0.56$). Nitrite-N concentrations steadily increased throughout sampling with a polynomial fit ($P < 0.0001$; $R^2 = 0.8319$). Initial NO_2^--N concentrations were 0 mg·L^{-1} at 4 HAI, increasing to 0.4 mg·L^{-1} at 8 HAI and continuing to increase to 4.4 mg·L^{-1} at 48 HAI, exhibiting a polynomial fit ($P < 0.001$; $R^2 = 0.83$) (Fig. 4). Nitrate-N concentrations were low during the first 8 h; they increased from 0.3 mg·L^{-1} at 4 HAI to 14.7 mg·L^{-1} at 48 HAI and were characterized by a polynomial fit ($P < 0.0001$; $R^2 = 0.9496$). The sum of all inorganic N

Downloaded from https://prime-pdf-watermark.prime-prod.pubfactory.com/ at 2025-08-15 via Open Access. This is an open access article distributed under the CC BY-NC license (https://creativecommons.org/licenses/by-nc/4.0/). https://creativecommons.org/licenses/by-nc/4.0/

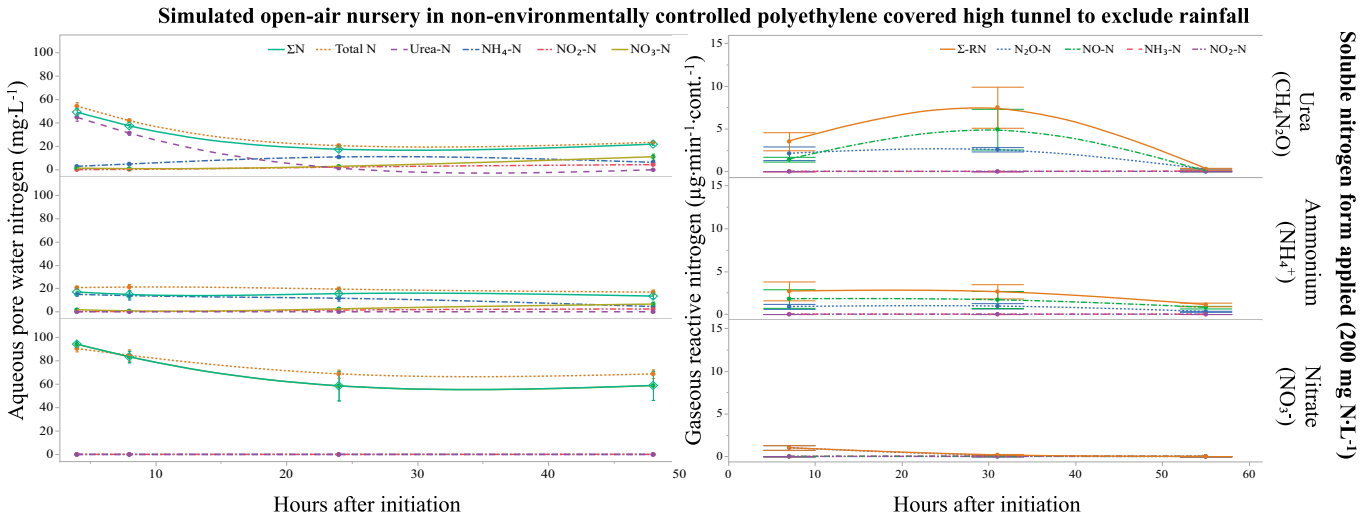

Fig. 2. Aqueous pore water nitrogen (N) via pour-through extraction (n = 4) and gaseous reactive N via Fourier transform infrared spectroscopy (n = 4) over time after applying water-soluble forms of urea (CH_4N_2O), ammonium phosphate [$(NH_4)H_2PO_4$], or potassium nitrate (KNO_3) to containerized (5.7 L) pine bark with an established shrub rose established in a nonenvironmentally controlled double-walled polyethylene-covered high tunnel to exclude rainfall but simulate an open-air nursery. Pore water aqueous species (left column) include the sum of N species or dissolved inorganic N (ΣN), total combustible N (TN), and N contributed from urea (CH_4N_2O), ammonium (NH_4^+), nitrite (NO_2^-), and nitrate (NO_3^-). Gaseous reactive N species (right column) include the sum of N reactive species (Σ-RN) and N contributed from nitrous oxide (N_2O), ammonia (NH_3), nitric oxide (NO), or nitrogen dioxide (NO_2). Inert nitrogen gas (N_2) was not measured.

concentrations was initially low, with a concentration of 1.2 mg·L^{-1} at 4 HAI, which increased to 64.8 mg·L^{-1} at 8 HAI and then decreased to 57.4 mg·L^{-1} at 24 HAI and 38.4 mg·L^{-1} at 48 HAI (Fig. 4). The CH_4N_2O-N treatment EC values did not change over time with this treatment (Fig. 5). The CH_4N_2O-N treatment pore water TOC remained relatively stable throughout the experiment, with an average of 89.2 mg·L^{-1} (Supplemental Fig. 8).

Gaseous emissions. Nitrous oxide-N emission concentrations were initially high at 7 HAI, with a concentration of 2.1 μg·min^{-1}, peaked at 31 HAI at 2.6 μg·min^{-1}, and then decreased to 0.3 μg·min^{-1} at 55 HAI, thus expressing a polynomial fit (P = 0.0189; R^2 = 0.5862) (Fig. 4). Nitric oxide-N emissions were 1.4 μg·min^{-1} at 7 HAI and peaked 31 HAI at 4.9 μg·min^{-1}; however, the values were not statistically significant (P = 0.573). There were no emissions of NO-N at 55 HAI (Fig. 4). Nitric oxide and N_2O (NO-N and N_2O-N) were the two major contributors to RN emissions regardless of sampling time. Minor emissions of NH_3-N were measured at 55 HAI, with a value of 0.04 μg·min^{-1}, while there were no emissions of NO_2-N at any point during the experimental sampling for this treatment (Fig. 4).

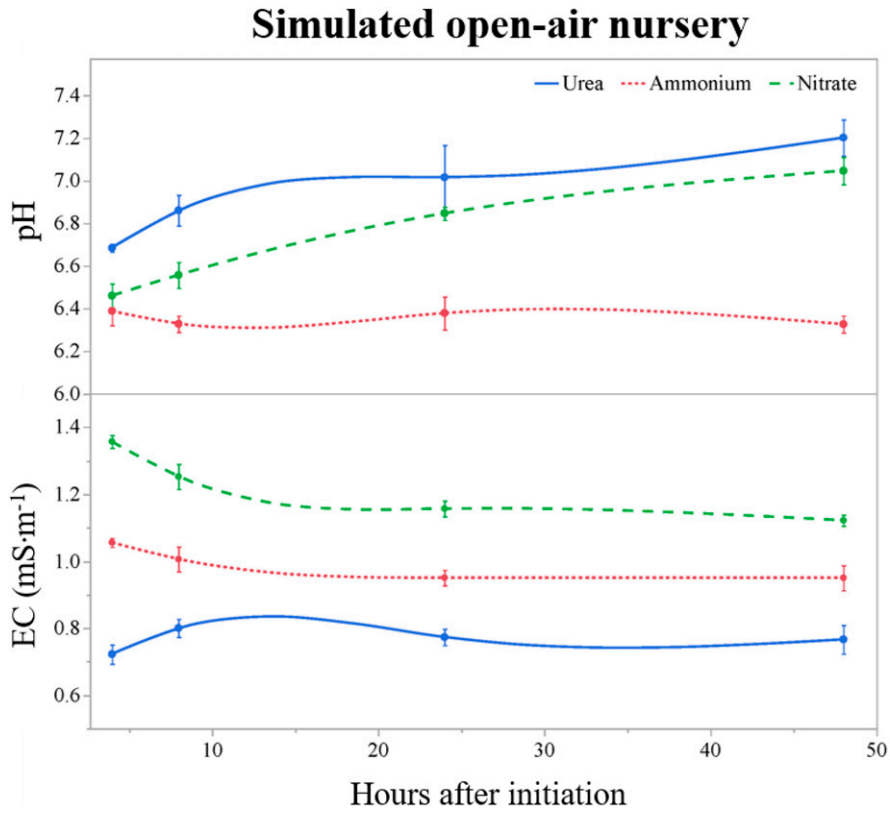

Fig. 3. Pore water pH (upper panel) and electrical conductivity (EC; lower panel) via pour-through extraction over time after applying water-soluble forms of urea (CH_4N_2O), ammonium phosphate [$(NH_4)H_2PO_4$], or potassium nitrate (KNO_3) to containerized (5.7 L) pine bark with an established shrub rose established in a nonenvironmentally controlled double-walled polyethylene-covered high tunnel to exclude rainfall but simulate an open-air nursery. Vertical bars indicate the standard error.

Ammonium treatment

Aqueous pore water. Following the NH_4^+-N application, NH_4^+-N concentrations were initially 1.6 mg·L^{-1} at 4 HAI, increased to and peaked at 24 HAI at 62.4 mg·L^{-1}, and then decreased to 56.1 mg·L^{-1} at 48 HAI, thus exhibiting a polynomial fit ($P < 0.0001$; R^2 = 0.74) Fig. 4). Aqueous NO_2^--N exhibited a polynomial fit ($P < 0.0001$; R^2 = 0.92) (Fig. 4). The concentrations were low during the first 24 HAI (>0.2 mg·L^{-1}) and then increased to 1.6 mg·L^{-1} at 48 HAI. The sum of all inorganic N concentrations was initially 3.8 mg·L^{-1} at 4 HAI and increased to 68.3 mg·L^{-1} at 48 HAI (Fig. 4). Urea-N was not present at any sampling point for the NH_4^+-N treatment (Fig. 4). The NH_4^+-N treatment pore water pH decreased by 0.5 units from 6.6 at 4 HAI to 6.1 at 48 HAI (P = 0.0153) (Fig. 5). The NH_4^+-N treatment pore water EC (mS·cm^{-1}) remained relatively stable for the entirety of the experiment (Fig. 5). The TOC concentration remained stable throughout the experiment, increasing from 57.8 mg·L^{-1} at 4 HAI to 65.0 mg·L^{-1} at

Downloaded from https://prime-pdf-watermark.prime-prod.pubfactory.com/ at 2025-08-15 via Open Access. This is an open access article distributed under the CC BY-NC license (https://creativecommons.org/licenses/by-nc/4.0/). https://creativecommons.org/licenses/by-nc/4.0/

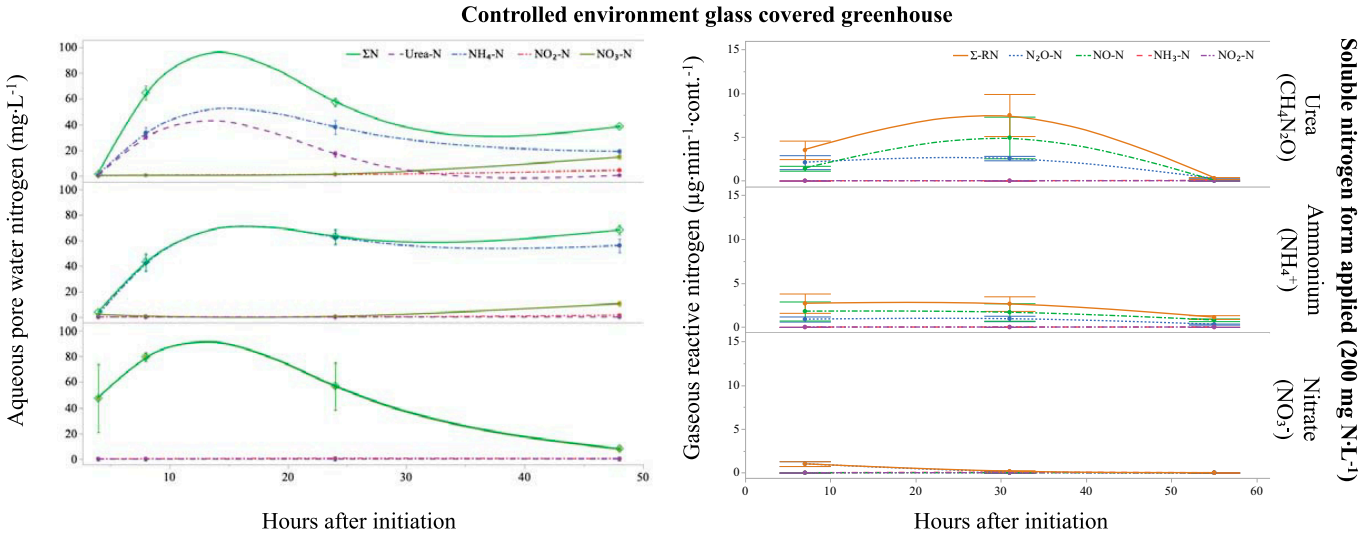

Fig. 4. Aqueous pore water nitrogen (N) via pour-through extraction (n = 4) and gaseous reactive N via Fourier transform infrared spectroscopy (n = 4) over time after applying water-soluble forms of urea (CH_4N_2O), ammonium phosphate [$(NH_4)H_2PO_4$], or potassium nitrate (KNO_3) to containerized (5.7 L) pine bark with an established shrub rose in an environmentally controlled glass greenhouse. Pore water aqueous species (left column) include the sum of N species or dissolved inorganic N (ΣN) and N contributed from urea (CH_4N_2O), ammonium (NH_4^+), nitrite (NO_2), and nitrate (NO_3^-). Gaseous reactive N species (right column) include the sum of N reactive species (Σ-RN) and N contributed from nitrous oxide (N_2O), ammonia (NH_3), nitric oxide (NO), or nitrogen dioxide (NO_2). Inert nitrogen gas (N_2) was not measured.

48 HAI (P = 0.322) (Supplemental Fig. 8); however, it exhibited no significant difference.

Gaseous emissions. The NH_4^+-N treatment showed a similar trend of N_2O-N emission concentrations as the CH_4N_2O-N treatment, although to a lesser extent, increasing from 0.9 µg·min^{-1} at 7 HAI to 1.0 µg·min^{-1} at 31 HAI and decreasing to 0.3 µg·min^{-1} at 55 HAI (P = 0.1372) (Fig. 4). Nitric oxide-N emission concentrations remained stable with only minor changes during the experiment (P = 0.4049) (Fig. 4). Nitric and nitrous oxide (NO-N and N_2O-N) were the two major contributors to RN emissions regardless of sampling time. There were no measured emissions of NH_3-N and NO_2-N at any sampling point during the experimental sampling (Fig. 4).

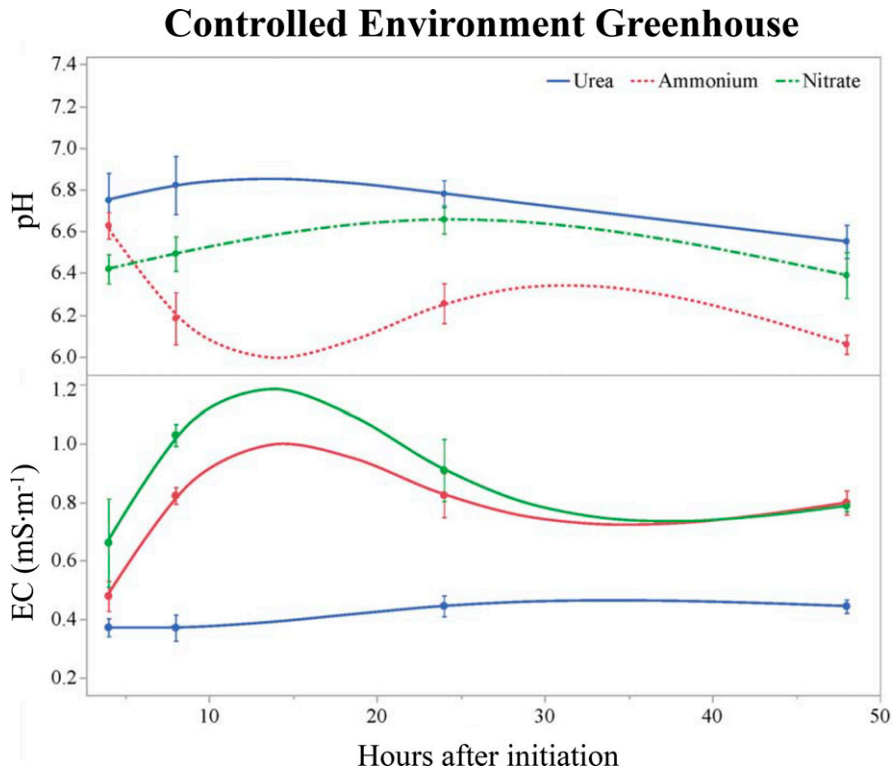

Fig. 5. Pore water pH (upper panel) and electrical conductivity (EC; lower panel) via pour-through extraction over time after applying water-soluble forms of urea (CH_4N_2O), ammonium phosphate [$(NH_4)H_2PO_4$], or potassium nitrate (KNO_3) to containerized (5.7 L) pine bark with and shrub rose established in a controlled environment glass greenhouse. Vertical bars indicate the standard error.

Nitrate treatment

Aqueous pore water. Following the application of NO_3^--N fertilizer, NO_3^--N concentrations were 47.4 mg·L^{-1} 4 HAI, peaked at 8 HAI at 79.4 mg·L^{-1}, and decreased to 7.7 mg·L^{-1} at 48 HAI (P = 0.026) (Fig. 4). Nitrite-N concentrations remained stable during the experiment (Fig. 4). Ammonium-N and CH_4N_2O-N remained below detection limits for all sampling points (Fig. 4). The sum of all inorganic N concentrations was initially 47.5 mg·L^{-1} at 4 HAI, increased at 8 HAI with a concentration of 79.6 mg·L^{-1}, and decreased to 8.2 mg·L^{-1} at 48 HAI (Fig. 4). The pH of the pore water when fertilized with the NO_3^--N treatment remained stable throughout the experimental sampling (P = 0.7533) (Fig. 5). The EC (mS·m^{-1}) of the pore water solution of the NO_3^--N treatment was stable throughout sample collection (P = 0.8785) (Fig. 5). The TOC concentrations (mg·L^{-1}) increased over the experiment from an initial value of 54 mg·L^{-1} at 4 HAI to 82.1 mg·L^{-1} at 48 HAI, exhibiting a polynomial fit (P = 0.0361; R^2 = 0.40) (Supplemental Fig. 8).

Gaseous emissions. Nitrous oxide-N (N_2O) emission exhibited a polynomial fit (P = 0.0032; R^2 = 0.72); concentrations of 1.0 µg·min^{-1} from the NO_3^--N treatment were the highest at 7 HAI and then decreased to 0.1 µg·min^{-1} at 31 HAI and <0.1 µg·min^{-1} at 55 HAI (Fig. 4). Low emissions of NH_3-N occurred at 31 HAI, with a concentration of 0.1 µg·min^{-1}. However, no emissions of this species occurred at 7 HAI or 55 HAI. There were no emissions of NO-N and NO_2-N during any sample collection.

Downloaded from https://prime-pdf-watermark.prime-prod.pubfactory.com/ at 2025-08-15 via Open Access. This is an open access article distributed under the CC BY-NC license (https://creativecommons.org/licenses/by-nc/4.0/). https://creativecommons.org/licenses/by-nc/4.0/

Discussion

The objective of this research was to determine the reactions and transformations of applied single N sources (CH_4N_2O-N, NH_4^+-N, or NO_3^--N) in a container-grown crop (pine bark substrate) microbiome in either a high tunnel or the controlled environment of a glass greenhouse to elucidate N reactions and transformations. Our data directly and inferentially illustrated the various aqueous and gaseous dynamic enzymatic and microbial transformations of the container biome involving urea hydrolysis, nitrification, and denitrification by regularly measuring applied and intermediate forms of N in aqueous and gaseous phases over a 2-day production setting. The microbiome was not analyzed.

Reaction sequence informed by gaseous and aqueous reactions

Urea application. Urea hydrolysis, conversion of CH_4N_2O-N to NH_4^+-N, occurred in both the high tunnel and glass greenhouse regardless of environment. The highest emissions of RN gases occurred in the CH_4N_2O-N treatment; this indicated that most gaseous RN species formations appear to stem from CH_4N_2O-N hydrolysis and subsequent nitrification of NH_4^+-N to NO_3^--N, while denitrification, anaerobic reduction of NO_3^--N to downstream gaseous species, seems to be a lesser contributor to RN emissions (Figs. 2 and 4). After applying CH_4N_2O-N, NH_4^+-N increased and by-products of nitrification-mediated reactions that include increased NO_2^--N and NO_3^--N (Figs. 2 and 4) were observed. We inferred that aqueous NO_2^--N formation was brief and resulted in the rapid and complete nitrification of NO_2^--N to NO_3^--N because the NO_3^--N:NO_2^--N ratio was greater than one. Initial pH increased because CH_4N_2O hydrolysis during the first 24 HAI occurred as expected (Niemiera et al. 2014); thereafter, pH was stable for the remainder of the high tunnel experiment. We attributed this result to concurrent nitrification reactions (acidic) and denitrification reactions (alkaline) (Figs. 3 and 5). The changes in pH were less prevalent in the glass greenhouse (Fig. 5), likely because of a more stable pH as a result of a less variable environment that may have slowed the reaction rate. Our results indicated that applied CH_4N_2O-N is predominately and completely hydrolyzed within 48 h of application (Figs. 2 and 4). These results are similar to those found by Niemiera et al. (2014).

Ammonium application. A steady decrease of NH_4^+-N and a concomitant increase in aqueous NO_2^--N and NO_3^--N regardless of a high-tunnel or glass greenhouse setting indicated a rapid rate of nitrification as previously shown by Niemiera and Wright (1987a) (Fig. 2). We inferred that nitrification and denitrification occurred concurrently when NH_4^+-N was applied because of the observed stable pH throughout sampling as previously described (Figs. 3 and 5). A less pronounced decrease in NH_4^+-N and an increase in NO_3^--N were observed when CH_4N_2O-N was applied to containers in the glass greenhouse (Fig. 4). Similar to when NO_3^--N was applied, the decreased degrees of NH_4^+-N and NO_3^--N changes were attributed to greater temperature control in the greenhouse lessening temperature extremes and decreased evapotranspiration and subsequent of solute flux. When applying NH_4^+-N, products of nitrification NO_2^--N and NO_3^--N were found throughout pore water sampling in increasing concentrations over time (Figs. 2 and 4).

Nitrate application. In both the high tunnel and glass greenhouse, when NO_3^--N was applied, there was a steady decrease of NO_3^--N without the presence of any other N intermediate aqueous species (Figs. 2 and 4). Denitrification resulted in lower emissions of RN from the NO_3^--N treatments (Figs. 2 and 4). This lack of N intermediaries implied that denitrification is the major N transformation resulting in the formations of N_2 gas (not measured). The decrease in NO_3^--N coupled with an increasing pH (Figs. 3 and 5) implicated the alkaline nature of denitrification (Havlin et al. 2014) that occurred after the application of NO_3^--N.

Synthesis. Regardless of the N source applied, or whether the environment was uncontrolled or controlled, the trend of reactions included the formation of NH_4^+-N via CH_4N_2O hydrolysis and then NO_3^--N via nitrification, which resulted in denitrification and the inferred complete denitrification to N_2. Thus, our findings suggested that these reactions proceed in a reaction sequence from CH_4N_2O hydrolysis to nitrification to denitrification, depending on the applied N form (Fig. 6). The formation of aqueous NO_2^--N appeared to be associated with nitrification from NH_4^+-N application or hydrolyzed CH_4N_2O-N and was ephemerally formed via denitrification because of the low concentrations measured from the application of NO_3^--N (Figs. 2 and 4). Aqueous NO_2^--N formation in the denitrification reaction appeared to be readily transformed into gaseous N species shown by low NO_2^--N concentrations in pore water sampling (Figs. 2 and 4).

Numerous microbial communities can use the applied N in the substrate to form predominately N_2 or lesser losses of RN gaseous intermediates (NO-N, N_2O-N, and NH_3-N) of nitrification and denitrification (Caranto and Lancaster 2017). Regarding applied N fertilizers, gaseous losses have been found to be nearly equivalent to aqueous losses via leaching according to previous research (Brown 2024). Urea resulted in higher RN gaseous emissions than those of the NO_3^--N treatment. In contrast, NH_4^+-N treatment emissions were the same when compared with CH_4N_2O-N and NO_3^--N treatments (Figs. 2 and 4). Based on these results, we inferred that the gaseous losses from the NO_3^--N treatment were more likely in the form of N_2 than RN gaseous species N_2O-N, NO-N, and NH_3-N. Denitrification appears to be the final reaction of applied N because all processes after application in our system resulted in increasing concentrations of NO_3^--N.

Nitrogen inefficiencies in production. We inferred from these data that using CH_4N_2O-N based fertilizers resulted in greater losses of RN gaseous emission compared with NO_3^--N-based fertilizer products. The application and use of NO_3^--N-based fertilizers may reduce greenhouse gases emissions from N fertilizers and more readily form the relatively inert N_2 species.

Neither plant N nor substrate-bound N was affected by the applied N source. We attributed the lack of plant N uptake and N substrate sorption to the introduction of N during establishment, the relatively short treatment exposure of 48 h, and analytical sampling sensitivity. These results support previous findings that denitrification resulting in N_2 gas formation is a major, if not the predominant, inefficiency when applying N fertilizers (Pitton et al. 2022). Although these losses may be economically concerning to growers, gaseous losses of N from containerized cropping systems may present less harmful RN gaseous emissions in container-grown crops in the United States than previously hypothesized by Pitton et al. (2022). However, RN losses or emissions on larger scales may result in considerable economic and environmental losses.

Future considerations. Havlin et al. (2014) noted that the emission of N_2 via denitrification in commercially produced container-grown plants appeared to be a rapid process. Management practices that may have the capability to slow or stabilize applied forms of N or the release of N to the production system should be investigated. However, attempting to alter natural enzymatic or microbially aided processes, as present in N cycle transformations, may produce losses of other forms of N, as noted by Souza et al. (2023). Dinitrogen gas formation from applied fertilizers is a loss of fertilizer economic expenditures to growers; however, this N gaseous species is inert and the primary gas composing the atmosphere (approximately 78%). Fertilizer N not used by the plant or bound to substrate and subsequently lost as N_2 may be the best-case scenario because N_2 has no associated environmental or health-related consequences (Scheer et al. 2020).

As the mechanisms of nutrient release from N-containing controlled-release fertilizers continue to improve, researchers may be tasked with revisiting best management practices coupled with economic research to attempt to reduce inputs and labor costs that may relieve some of the financial and environmental pressures faced by the green industry (Fulcher et al. 2016). By improving fertilizer application, nutrient release, and longevity, N efficiency could be improved.

Products that claim to inhibit transformations of applied N forms and thereby mitigate aqueous and gaseous losses are currently being sold and marketed to the nursery industry; however, in a recent publication by Souza et al. (2023), some of these products have unintended consequences. When using some of these inhibition products, mitigated losses of N were offset by increased RN gas emissions, specifically N_2O-N, and leachate losses of NO_3^--N. By working with simulated conditions and investigating fertilizer and irrigation

Downloaded from https://prime-pdf-watermark.prime-prod.pubfactory.com/ at 2025-08-15 via Open Access. This is an open access article distributed under the CC BY-NC license (https://creativecommons.org/licenses/by-nc/4.0/). https://creativecommons.org/licenses/by-nc/4.0/

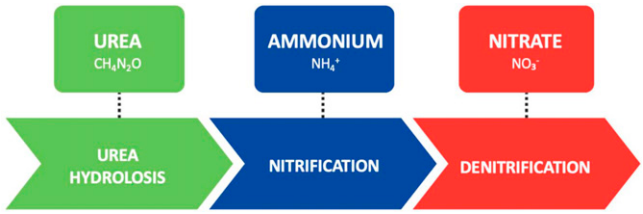

Fig. 6. Initial and subsequent reaction sequence based on the applied nitrogen source in a containerized cropping system.

applications, as well as various other management practices, alternative cultural practices may be developed to improve N application and retention without the need for additional chemistries in the container throughout the production cycle.

Limitations within research. A significant limitation within the scope of the N fate and gaseous emission of N is our inability to directly measure N_2 losses. Currently, analytical techniques are less effective for measuring N_2 emissions compared with many other gaseous species of interest; this is attributed to the use of N_2 in the sampling apparatus or high background atmospheric levels of N2 (Takaya et al. 2003). Until N_2 can be effectively and efficiently measured, skepticism about the applied N fate in a production system will remain a topic for debate.

Conclusions

Our results indicated that within the pine bark-filled container there is a suite of dynamic chemical, enzymatic, and microbial reactions that take place within the substrate pore water that are dependent on the N source applied. The application of urea results in rapid urea hydrolysis followed by concurrent and consecutive nitrification and denitrification, while the application of ammonium results in nitrification and denitrification. The application of nitrate results in denitrification.

References Cited

Akiyama H, Tsuruta H. 2003. Nitrous oxide, nitric oxide, and nitrogen dioxide fluxes from soils after manure and urea application. J Environ Qual. 32(2):423–431. https://doi.org/10.2134/jeq2003.4230.

Alam MZ, Chong C, Llewellyn J, Lumis GP. 2009. Evaluating fertilization and water practices to minimize NO3-N leachate from container-grown forsythia. HortScience. 44(7):1833–1837. https://doi.org/10.21273/HORTSCI.44.7.1833.

Altland JE, Locke JC, Krause CR. 2014. Influence of pine bark particle size and pH on cation exchange capacity. HortTechnology. 24(5):554–559. https://doi.org/10.21273/HORTTECH.24.5.554.

Altland JE, Owen JS Jr, Jackson BE, Fields JS. 2018. Physical and hydraulic properties of commercial pine-bark substrate products used in production of containerized crops. HortScience. 53(12):1883–1890. https://doi.org/10.21273/HORTSCI13497-18.

Altland JE, Owen JS Jr. 2024. The pour-through procedure preferentially extracts substrate solution from the bottom of the container in conventional and stratified substrates. HortScience. 59(2):201–208. https://doi.org/10.21273/hortsci17425-23.

Arnold MA, McDonald GV. 2006. Shrub rose responses to production in smart pots and conventional containers using two contrasting substrates. J Rio Grande Val Hortic Soc. 58:1–4.

Bilderback TE, Fonteno W. 1987. Effects of container geometry and media physical properties on air and water volumes in containers. J Environ Hortic. 5(4):180–182. https://doi.org/10.24266/0738-2898-5.4.180.

Bilderback T, Boyer C, Chappell M, Fain G, Fare D, Gilliam C, Jackson B, Lea-Cox J, LeBude A, Niemiera A, Owen J Jr, Ruter J, Tilt K, Warren S, White S, Whitwell T, Wright R, Yeager T. 2015. Best management practices: guide for producing nursery crops (3rd ed). Southern Nursery Association, Acworth, GA, USA.

Brown F. 2024. Nitrogen fate and transformations in the production of specialty containerized crops. (PhD Diss). Virginia Polytechnic Institute and State University, Blacksburg, VA, USA.

Caranto JD, Lancaster KM. 2017. Nitric oxide is an obligate bacterial nitrification intermediate produced by hydroxylamine oxidoreductase. Proc Natl Acad Sci USA. 114(31):8217–8222. https://doi.org/10.1073/pnas.1704504114.

Cavins TJ, Whipker BE, Fonteno WC. 2005. Pourthru: A method for monitoring nutrition in the greenhouse. International Symposium on Growing Media. 779:289–298.

Chen J, Wei X. 2018. Controlled-release fertilizers as a means to reduce nitrogen leaching and runoff in container-grown plant production. Nitrogen in agriculture - Updates. InTech. 33–52.

Congreves KA, Otchere O, Ferland D, Farzadfar S, Williams S, Arcand M. 2021. Nitrogen use efficiency definitions of today and tomorrow. Front Plant Sci. 12:1–10. https://doi.org/10.3389/fpls.2021.637108.

Fonteno WC, Harden CT. 2010. North Carolina State University horticultural substrates lab manual. North Carolina State University, Raleigh, NC, USA. 49(6):827–832.

Fulcher A, LeBude AV, Owen JS Jr, White SA, Beeson RC. 2016. The next ten years: Strategic vision of water resources for nursery producers. HortTechnology. 26(2):121–132. https://doi.org/10.21273/HORTTECH.26.2.121.

Galloway JN, Dentener FJ, Capone DG, Boyer EW, Howarth RW, Seitzinger SP, Asner GP, Cleveland CC, Green PA, Holland EA, Karl DM, Michaels AF, Porter JH, Townsend AR, Vöosmarty CJ. 2004. The nitrogen cascade. Biogeochemistry. 70(2):153–226. https://doi.org/10.1007/s10533-004-0370-0.

Govindasamy P, Muthusamy SK, Bagavathiannan M, Mowrer J, Jagannadham PTK, Maity A, Halli HM, G K S, Vadivel R, T K D, Raj R, Pooniya V, Babu S, Rathore SS, L M, Tiwari G. 2023. Nitrogen use efficiency—a key to enhance crop productivity under a changing climate. Front Plant Sci. 14:1121073. https://doi.org/10.3389/fpls.2023.1121073.

Gyawali AJ, Lester BJ, Stewart RD. 2019. Talking SMAAC: A new tool to measure soil respiration and microbial activity. Front Earth Sci. 7(138):1–8.

Havlin JL, Tisdale SL, Nelson WL, Beaton JD. 2014. Soil fertility and fertilizers: An introduction to nutrient management. Pearson Higher Ed, Upper Saddle River, NJ, USA.

Hoskins TC, Owen JS Jr, Niemiera AX. 2014a. Controlled-release fertilizer placement affects the leaching pattern of nutrients from nursery containers during irrigation. HortScience. 49(10):1341–1345. https://doi.org/10.21273/HORTSCI.49.10.1341.

Hoskins TC, Owen JS Jr, Niemiera AX. 2014b. Water movement through a pine-bark substrate during irrigation. HortScience. 49(11):1432–1436. https://doi.org/10.21273/HORTSCI.49.11.1432.

Kroeze C, Mosier A, Bouwman A. 1999. Closing the global NO2 budget: A retrospective analysis 1500-1994. Global Biogeochem. Cycles. 13(1):1–8.

Li T, Bi G, Harkess RL, Denny GC, Scagel C. 2019. Nitrogen fertilization and irrigation frequency affect hydrangea growth and nutrient uptake in two container types. HortScience. 54(1):167–174. https://doi.org/10.21273/HORTSCI13513-18.

Mack R, Owen JS Jr, Niemiera AX, Latimer J. 2017. Virginia nursery and greenhouse grower survey of best management practices. HortTechnology. 27(3):386–392. https://doi.org/10.21273/HORTTECH03664-17.

Majsztrik J, Ristvey AG, Lea-Cox J. 2010. Water and nutrient management in the production of container-grown ornamentals, p 253–297. In: Janick J (ed). Horticultural Reviews.

Marschner P. 2012. Marschner's mineral nutrition of higher plants. Academic Press, Cambridge, MA, USA.

Matassa S, Boeckx P, Boere J, Erisman JW, Guo M, Manzo R, Meerburg F, Papirio S, Pikaar I, Rabaey K, Rousseau D, Schnoor J, Smith P, Smolders E, Wuertz S, Verstraete W. 2023. How can we possibly resolve the planet's nitrogen dilemma? Microb Biotechnol. 16(1):15–27. https://doi.org/10.1111/1751-7915.14159.

Million JB, Yeager TH. 2022. Fabric containers increased irrigation demand but decreased leachate loss of nitrogen and phosphorus compared with conventional plastic containers during production of Dwarf Burford Holly. HortScience. 57(7):743–749. https://doi.org/10.21273/HORTSCI16570-22.

Myhre G, D, Shindell F-M, Bréon W, Collins J, Fuglestvedt J, Huang D, Koch J-F, Lamarque D, Lee B, Mendoza T, Stocker D, Qin G-K, Plattner M, Tignor S, Allen J, Boschung. 2013. Climate Change 2013: The Physical Science Basis. Contribution of Working Group I to the Fifth Assessment Report of the Intergovernmental Panel on Climate Change. Cambridge University Press, Cambridge, UK.

Niemiera AX, Wright RD. 1987a. Influence of temperature on nitrification in a pine bark medium. HortScience. 22(4):615–616. https://doi.org/10.21273/HORTSCI.22.4.615.

Niemiera AX, Wright RD. 1987b. Influence of NH_4-N application rate on nitrification in a pine bark medium. HortScience. 22(4):616–618. https://doi.org/10.21273/HORTSCI.22.4.616.

Niemiera AX, Taylor LL, Shreckhise JH. 2014. Urea hydrolysis in pine tree substrate is affected by urea and lime rates. HortScience. 49(11):1437–1443. https://doi.org/10.21273/HORTSCI.49.11.1437.

Downloaded from https://prime-pdf-watermark.prime-prod.pubfactory.com/ at 2025-08-15 via Open Access. This is an open access article distributed under the CC BY-NC license (https://creativecommons.org/licenses/by-nc/4.0/). https://creativecommons.org/licenses/by-nc/4.0/

Pitton BJL, Oki L, Sisneroz J, Evans R. 2022. A nursery system nitrogen balance for production of a containerized woody ornamental plant. Sci Hortic. 291:110569–110567. https://doi.org/10.1016/j.scienta.2021.110569.

Pokorny FA. 1979. Pine bark container media—an overview. Proc Inti Plant Prop Soc. 29:484–494.

Scheer C, Fuchs K, Pelster DE, Butterbach-Bahl K. 2020. Estimating global terrestrial denitrification from measured N2O:(N2O+N2) product ratios. Sci Dir COSUST. 47:72–80. https://doi.org/10.1016/j.cosust.2020.07.005.

Souza EFC, Rosen CJ, Venterea RT, Tahir M. 2023. Intended and unintended impacts of nitrogen-fixing microorganisms and microbial inhibitors on nitrogen losses in contrasting maize cropping systems. J Environ Qual. 52(5):972–983. https://doi.org/10.1002/jeq2.20500.

Takaya N, Catalan-Sakairi MA, Sakaguchi I, Kato Z, Zhou H, Shoun H. 2003. Aerobic denitrifying bacteria that produce low levels of nitrous oxide. Appl Environ Microbiol. 69(6):3152–3157. https://doi.org/10.1128/AEM.69.6.3152-3157.2003.

Theis S, Bruggeman S, Clay SA, Mishra U, Hatfield G, Kumar S, Clay DE. 2019. Mid-morning point sampling may not accurately represent nitrous oxide emissions following fertilizer applications. Soil Sci Soc Amer J. 83(2):339–347.

US Department of Agriculture–National Agricultural Statistics Service. 2020. 2017 Census of Agriculture, 2019 Census of horticultural specialties.

US Environmental Protection Agency. 2002. Nitrogen: Multiple and regional impacts.

Warsaw AL, Thomas Fernandez R, Kort DR, Cregg BM, Rowe B, Vandervoort C. 2012. Remediation of metalaxyl, trifluralin, and nitrate from nursery runoff using container-grown woody ornamentals and phytoremediation areas. Ecol Eng. 47:254–263. https://doi.org/10.1016/j.ecoleng.2012.06.036.

Wilson PC, Albano JP. 2011. Impact of fertigation versus controlled-release fertilizer formulations on nitrate concentrations in nursery drainage water. HortTechnology. 21(2):176–180. https://doi.org/10.21273/hortech.21.2.176.

Wright RD. 1986. The pour-through nutrient extraction procedure. HortScience. 21(2):227–229. https://doi.org/10.21273/hortsci.21.2.227.

Zheng Y. 2018. Current nutrient management practices and technologies used in North American greenhouse and nursery industries. Acta Hortic. 1227:435–442. https://doi.org/10.17660/actahortic.2018.1227.54.

Downloaded from https://prime-pdf-watermark.prime-prod.pubfactory.com/ at 2025-08-15 via Open Access. This is an open access article distributed under the CC BY-NC license (https://creativecommons.org/licenses/by-nc/4.0/). https://creativecommons.org/licenses/by-nc/4.0/